

## Benzene–Copper(I) Coordination in a Bimetallic Chain Complex

Andrew M. Dattelbaum and James D. Martin\*

Department of Chemistry, North Carolina State University, Raleigh, North Carolina 27695-8204

Received September 7, 1999

The solvothermal reaction of CuCl and ZrCl<sub>4</sub> in benzene yields ((bz)CuCl<sub>3</sub>)<sub>2</sub>Zr (**1**) (bz = η<sup>2</sup>-benzene), which has been characterized by single-crystal X-ray diffraction with *a* = 6.1206(4) Å, *b* = 11.1242(4) Å, *c* = 13.6222(6) Å, β = 93.675(3)° in the monoclinic space group *P*2<sub>1</sub>/*m*, *Z* = 2. **1** adopts a one-dimensional chain structure constructed from zirconium chloride octahedra and [(bz)CuCl<sub>3</sub>]<sup>2-</sup> tetrahedra. The [(bz)CuCl<sub>3</sub>]<sup>2-</sup> units are shown to be metal halide analogues of the phosphonate unit [RPO<sub>3</sub>]<sup>2-</sup>. Interchain interactions link chains of **1** along the crystallographic *c* direction via an edge-to-face π-stacking of the coordinated benzene molecules. The crystal packing forces influence dramatic second-order Jahn–Teller distortions, making each of the two ((bz)CuCl<sub>3</sub>)<sup>2-</sup> units distinct. These interactions further result in ligand-to-metal and metal-to-ligand charge transfers that cause an activation of the benzene ligands.

## Introduction

The synthesis and characterization of metalloorganic solids, in which organic ligands link metal centers, have received considerable attention as a means of designing specific supramolecular assemblies. Amine, cyanide, or organic acid ligands frequently serve as part of the scaffold for such frameworks. In our effort to develop open-framework metal halides, we are interested in developing the organometallic (as opposed to metallorganic) solid-state chemistry by incorporating extraframework organic ligands that can serve as active sites for catalysis. This model is patterned after the role of metal alkyls in Ziegler–Natta catalysis.<sup>1,2</sup> On the basis of our recently described strategy for preparing metal halide analogues of metal oxide structure types,<sup>3</sup> we have considered the preparation of metal halide analogues of the prolific class of metal phosphonates as a structural prototype for such organometallic solids. Both structurally and electronically, phosphonates (RPO<sub>3</sub>)<sup>2-</sup> can be related to (LCuCl<sub>3</sub>)<sup>2-</sup>, where L is a neutral ligand such as an olefin, aromatic, carbonyl, etc. Such organometallic solid-state chemistry finds structural precedence in (bz)CuAlCl<sub>4</sub><sup>4</sup> (bz = η<sup>2</sup>-benzene), which was not described in relation to this phosphonate analogy. In that material, benzene is bound to copper in an η<sup>2</sup>-fashion. Each copper is bridged through chlorides to aluminum forming a layered clay-type structure with the benzene ligands coordinated in the interlayer region. The benzene is readily lost from this layered structure to form α-CuAlCl<sub>4</sub>.<sup>5–7</sup> Interestingly, CuAlCl<sub>4</sub> is reported to catalyze the polymerization of benzene in the presence of oxygen.<sup>8</sup> And the insertion of CO into aromatic C–H bonds is reported to be catalyzed by CuCl and a strong Lewis acid such as AlCl<sub>3</sub>.<sup>9</sup> A

related chemistry could also be described for (bz)AgAlCl<sub>4</sub>, where the benzene is coordinated to a square pyramidal AgCl<sub>4</sub> unit of the AgAlCl<sub>4</sub> layers.<sup>10</sup> However, the silver to benzene interaction is reportedly weaker than the corresponding copper–benzene interaction.

Given the literature precedence for Cu(I) to reversibly bind unsaturated ligands, as well as its use as a cocatalyst with Lewis acids,<sup>6,7,11,12</sup> it seemed of interest to pursue the preparation of such phosphonate-type metal halide materials with copper chloride and other Lewis acidic metal halides. In this paper, we describe the preparation and characterization of ((bz)CuCl<sub>3</sub>)<sub>2</sub>Zr (**1**), a one-dimensional chain structure constructed from zirconium octahedra and copper tetrahedra. Chains of **1** are linked along the crystallographic *c* direction via an edge-to-face π-stacking of the coordinated benzene molecules. These crystal packing forces are shown to influence dramatic second-order Jahn–Teller distortions making each of the two ((bz)CuCl<sub>3</sub>)<sup>2-</sup> units distinct. The distortions of the distinct ((bz)CuCl<sub>3</sub>)<sup>2-</sup> units emphasize the unique donor and acceptor properties of the Cu(I) ion, which in turn result in differential activation of the aromatic ligands.

## Experimental Section

**General Procedures.** All reactions were performed under an inert atmosphere of dry N<sub>2</sub> in a glovebox or using Schlenk line techniques. ZrCl<sub>4</sub> (99.99%) was used as received from Aldrich. The CuCl was prepared from Cu metal and CuCl<sub>2</sub> (Aldrich) according to literature methods and further purified by sublimation.<sup>13</sup> Benzene (99.9%, Fisher) was distilled from Na/benzophenone and then stored under nitrogen and over molecular sieves. All powder X-ray diffraction measurements were obtained using an Enraf-Nonius Guinier camera and were indexed with respect to a silicon standard.

**Preparation of Cu<sub>2</sub>ZrCl<sub>6</sub> (**2**).** A sample of 0.2 mg of ZrCl<sub>4</sub> (0.858 mmol) and a sample of 0.14 mg of CuCl (1.72 mmol) were ground

- (1) Ziegler, K.; Holzkamp, E.; Breil, H. *Angew. Chem.* **1955**, *67*, 541.
- (2) Natta, G. *Macromol. Chem.* **1955**, *16*, 213.
- (3) Martin, J. D.; Dattelbaum, A. M.; Sullivan, R. M.; Thornton, T. A.; Wang, J.; Peachey, M. T. *Chem. Mater.* **1998**, *10*, 2699.
- (4) Turner R. W.; Amma, E. L. *J. Am. Chem. Soc.* **1966**, *88*, 1877.
- (5) Martin, J. D.; Leafblad, B. R.; Sullivan, R. M.; Boyle, P. D. *Inorg. Chem.* **1998**, *37*, 1341.
- (6) "Luminescent Materials" Ed. J. McKittrick; *Proc. Mater. Res. Soc.* **1999**, *560*, in press.
- (7) Sullivan, R. M.; Martin J. D. *J. Am. Chem. Soc.*, in press.
- (8) Toshima, N.; Kanaka, K.; Koshirai, A.; Hirai, H. *Bull. Chem. Soc. Jpn.* **1988**, *61*, 2551.

- (9) Gatterman, L.; Koch, H. *Chem. Ber.* **1897**, *30*, 1622.
- (10) Turner R. W.; Amma, E. L. *J. Am. Chem. Soc.* **1966**, *88*, 3243.
- (11) Hathaway, B. J. In *Comprehensive Coordination Chemistry*; Wilkinson, G., Gillard, R. D., McCleverty, J. A., Eds.; Pergamon: London, 1987; Vol. 5, Chapters 53.3.2.11, pp 568–571.
- (12) Karlin, K. D.; Gultneh, Y. *Prog. Inorg. Chem.* **1987**, *35*, 219.
- (13) Kauffman, G. B.; Fang, L. Y. *Inorg. Syn.* **1983**, *22*, 101.

together in a mortar and pestle and then transferred to a fused silica tube (6 mm i.d.  $\times$  8 cm). The reaction vessel was evacuated and sealed with a torch. The reaction was heated to 450 °C (above the melting point of CuCl) in a box furnace for 1 day, followed by cooling at 1.0 °C/min. A small temperature gradient in the furnace caused crystalline  $\text{Cu}_2\text{ZrCl}_6$  to sublime to the cool end of the tube in greater than 90% yield. Solution of the single-crystal X-ray structure is complicated by disorder and/or twinning and, thus, will be the subject of a subsequent paper.<sup>14</sup>

**Preparation of ((bz)CuCl<sub>3</sub>)<sub>2</sub>Zr (1).** A powdered sample of  $\text{Cu}_2\text{ZrCl}_6$  (0.15 mg, 0.0348 mmol) was placed in a thick-walled fused silica tube (10 mm o.d.  $\times$  6 mm i.d.). On a Schlenk line, 1.0 mL of benzene was added to the reaction vessel. The reaction mixture was frozen with liquid  $\text{N}_2$  and sealed using a torch such that the fused silica vessel was filled to 25% volume. The reaction mixture was heated to 150 °C for 1 week and then slowly cooled at a rate of 0.1 °C/min to yield a pale yellow crystalline solid (50% yield) from which a single crystal was isolated for an X-ray structure determination. (*Note of Caution: Upon heating the sealed reaction vessel significant pressures are generated that can lead to vessel rupture. Appropriate shielding should be utilized such as placing the reaction vessels in a capped iron pipe during heating.*) After the crystalline material is removed from the benzene solvent it gradually loses the coordinated benzene such that elemental analyses routinely exhibit a 20–25% loss of benzene for any given sample. Anal. Calcd for  $\text{C}_{12}\text{H}_{12}\text{Cl}_6\text{Cu}_2\text{Zr}$ : C, 24.04; H, 2.04. Found: (1) C, 17.20; H, 1.85; (2) C, 18.11; H, 1.60.

**X-ray Structure Determination of ((bz)CuCl<sub>3</sub>)<sub>2</sub>Zr (1).** A single crystal (0.28  $\times$  0.20  $\times$  0.14 mm) was mounted in a Pyrex capillary under a  $\text{N}_2$  atmosphere covered in silicone grease to decrease the loss of solvent. Single-crystal X-ray data were collected on an Enraf-Nonius CAD4 diffractometer at 298 K using Mo K $\alpha$  radiation ( $\lambda = 0.71073$  Å). Final cell constants were determined by a symmetry constrained fit of 24 well-centered reflections ( $35^\circ < 2\theta < 40^\circ$ ) and their Friedel pairs. A hemisphere of data,  $\pm h, \pm k, l$ , with 2108 unique reflections was collected by the  $\theta/2\theta$  scan mode out to  $\theta < 27^\circ$ . Data were scaled to the intensity check reflections using a five-point smoothing curve-fitting routine. An empirical absorption correction was applied using  $\psi$  scan data.

Systematic absences were found to be consistent with the space group  $P2_1/m$ , which was confirmed in the subsequent refinement. The structure was refined using the NRCVAX suite of programs.<sup>15</sup> All non-hydrogen atoms were located by direct methods using the SIR92 program<sup>16</sup> and refined anisotropically in the final refinement. Hydrogen atoms bound to the benzene rings were then added in calculated positions and assigned fixed temperature factors. A full-matrix least-squares calculation using the 1456 unique reflections ( $I > 1.0\sigma(I)$ ) gave a final refinement with  $R$  factors of  $R = 0.044$  and  $R_w = 0.054$ . The final difference map was flat with the largest peak ( $1.5 \text{ e}^-/\text{Å}^3$ ) located 0.968 Å from Cu(2).

**Extended Hückel calculations<sup>17</sup>** were performed on  $((\text{bz})\text{CuCl}_3)^{2-}$  fragments idealized from the crystal structure of **1**. Atomic and orbital parameters used were those from previously published works.<sup>18–20</sup> The Cu–Cl bond lengths were idealized to 2.3 Å, while the Cl–Cu–Cl angles were taken directly from the crystalline structure. Idealized benzene rings with C–C = 1.39 Å were made to interact with the  $(\text{CuCl}_3)^{2-}$  fragment using the two orientations and copper to benzene distances found in the crystal structure for Cu(1) and Cu(2), respectively.

## Results

A summary of crystallographic data for  $((\text{bz})\text{CuCl}_3)_2\text{Zr}$  (**1**) is given in Table 1 and selected bond distances and angles in

**Table 1.** Crystallographic Data for  $((\text{bz})\text{CuCl}_3)_2\text{Zr}$  (**1**)

formula	$(\text{C}_6\text{H}_6)_2\text{CuCl}_3)_2\text{Zr}$
formula wt (g/mol)	587.25
space grp (No.)	$P2_1/m$ (11)
color	yellow
$a$ (Å)	6.1206(4)
$b$ (Å)	11.1242(4)
$c$ (Å)	13.6222(6)
$\beta$ (deg)	93.675(3)
$V$ (Å <sup>3</sup> )	925.58(8)
$T$ (°C)	25
$Z$	2
$\rho_{\text{calcd}}$ (mg cm <sup>-3</sup> )	2.107
$\lambda$ (Mo K $\alpha$ ), Å	0.71073
$\mu$ (cm <sup>-1</sup> )	36.9
$R^a$	0.044
$R_w^b$	0.053
GOF <sup>c</sup>	1.56

<sup>a</sup>  $R_f = (\sum(F_o - F_c)/F_o)$ . <sup>b</sup>  $R_w = [\sum(w(F_o - F_c)^2)/\sum wF_o^2]^{1/2}$ . <sup>c</sup> GOF =  $[\sum(w(F_o - F_c)^2)/(\text{no. of reflns} - \text{no. of parameters})]^{1/2}$ .

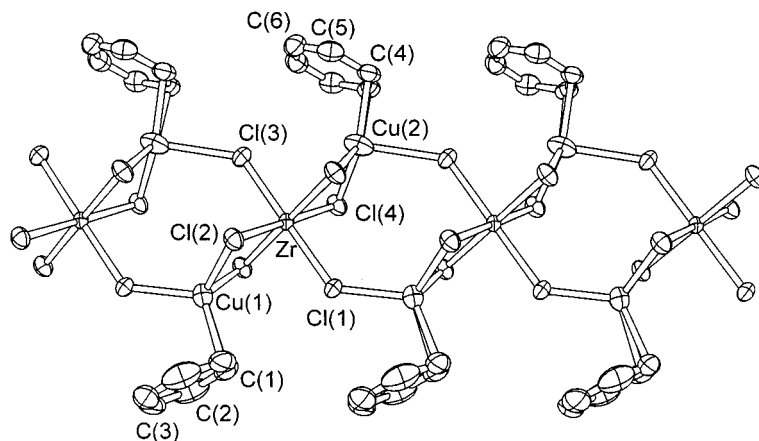
**Table 2.** Selected Bond Distances (Å) and Bond Angles (deg) for  $((\text{bz})\text{CuCl}_3)_2\text{Zr}$

Zr–Cu(1)	3.328(1)	Cu(1)–C(1)	2.306(7)
Zr–Cu(2)	3.222(2)	Cu(1)–X(1) <sup>a</sup>	2.205
		Cu(2)–C(4)	2.200(6)
Zr–Cl(1)	2.483(2)	Cu(2)–X(2) <sup>a</sup>	2.087
Zr–Cl(2) $\times$ 2	2.467(2)	C(1)–C(1')	1.35(2)
Zr–Cl(3)	2.436(2)	C(1)–C(2)	1.39(1)
Zr–Cl(4) $\times$ 2	2.485(2)	C(2)–C(3)	1.37(1)
		C(3)–C(3')	1.35(2)
Cu(2)–Cl(3)	2.664(3)	C(4)–C(4')	1.39(1)
Cu(2)–Cl(4)	2.335(2)	C(4)–C(5)	1.40(1)
Cu(2)–Cl(4)	2.335(2)	C(5)–C(6)	1.35(1)
Cu(1)–Cl(1)	2.325(2)	C(6)–C(6')	1.39(2)
Cu(1)–Cl(2)	2.403(2)		
Cu(1)–Cl(2)	2.403(2)		
Cl(1)–Zr–Cl(2)	89.06(5)	Cl(1)–Cu(1)–Cl(2)	110.99(6)
Cl(1)–Zr–Cl(2)	89.06(5)	Cl(2)–Cu(1)–Cl(2)	94.24(6)
Cl(1)–Zr–Cl(3)	179.65(8)	Cl(3)–Cu(2)–Cl(4)	101.10(6)
Cl(1)–Zr–Cl(4)	90.43(5)	Cl(4)–Cu(2)–Cl(4)	96.38(7)
Cl(1)–Zr–Cl(4)	90.43(5)		
Cl(2)–Zr–Cl(3)	91.18(5)	Cl(1)–Cu(1)–C(1)	113.2(2)
Cl(2)–Zr–Cl(4)	178.79(6)	Cl(2)–Cu(1)–C(1)	98.5(2)
Cl(3)–Zr–Cl(4)	89.32(6)	Cl(3)–Cu(2)–C(4)	90.6(2)
		Cl(4)–Cu(2)–C(4)	111.6(2)
Zr–Cl(1)–Cu(1)	130.5(1)	C(1)–C(1')–C(2)	119.5(7)
Zr–Cl(2)–Cu(1)	86.23(5)	C(1)–C(2)–C(3)	120.5(8)
Zr–Cl(3)–Cu(2)	132.7(1)	C(2)–C(3)–C(3')	120.0(7)
Zr–Cl(4)–Cu(2)	83.81(6)		
Cu(1)–Zr–Cu(2)	174.92(4)	C(4)–C(4')–C(5)	119.8(6)
		C(4)–C(5)–C(6)	119.4(7)
		C(5)–C(6)–C(6')	120.8(6)

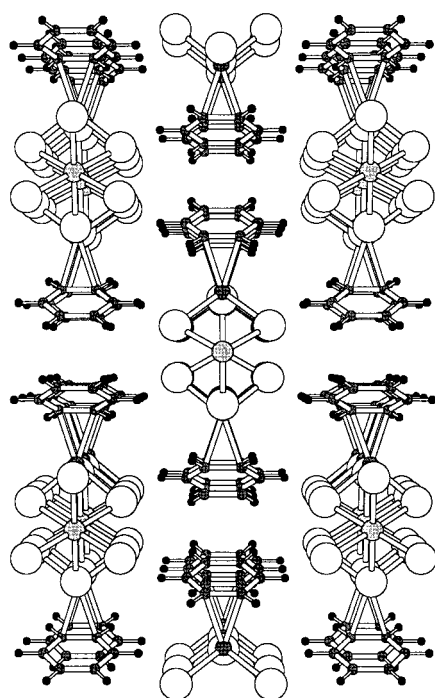
<sup>a</sup> X = midpoint of the C–C bond bound to its respective copper atom.

Table 2. An ORTEP drawing of the 1-D chain structure of **1** is shown in Figure 1, and a view of the unit cell looking down  $a$  is given in Figure 2. The structure of **1** consists of chains running along  $a$  in which the phosphonate-like tetrahedral units,  $((\text{bz})\text{CuCl}_3)^{2-}$ , are linked by  $\text{Zr}^{4+}$  cations. The chains lie across the mirror plane such that two pairs of chloride ligands (Cl(2) and Cl(2') and Cl(4) and Cl(4')) bridge the copper tetrahedra and zirconium octahedra resulting in common edges of the polyhedra. The additional chloride ligands bridge vertexes of the copper tetrahedra and zirconium octahedra. The two  $(\text{bz})\text{CuCl}_3$  units are notably distinct, moved away from being related through an approximate center of inversion by interchain edge-to-face  $\pi$ -stacking of the benzene ligands (discussed below).

- (14) Dattelbaum, A. M.; Martin, J. D. To be published.  
 (15) Gabe, E. J.; Le Page, Y.; Charland, J.-P.; Lee, F. L.; White, P. S. J. *Appl. Crystallogr.* **1989**, *22*, 384.  
 (16) Altomare, A.; Burla, M. C.; Camullini, G.; Cascarano, G.; Giacovazzo, C.; Guagliardi, A.; Polidori, G. *J. Appl. Crystallogr.* **1994**, *27*, 435.  
 (17) Hoffman, R. D. *J. Chem. Phys.* **1963**, *39*, 1397.  
 (18) Ammeter, J. H.; Bürgi, H.-B.; Thibeault, J. C.; Hoffman, R. J. *J. Am. Chem. Soc.* **1978**, *100*, 3686.  
 (19) Hay, P. J.; Thibeault, J. C.; Hoffman, R. J. *J. Am. Chem. Soc.* **1975**, *97*, 4884.  
 (20) Summerville, R. H.; Hoffman, R. J. *J. Am. Chem. Soc.* **1976**, *98*, 7240.



**Figure 1.** ORTEP drawing of the chains in  $((bz)CuCl_3)_2Zr(1)$  running along **a**. Thermal displacement ellipsoids are drawn at 50%.



**Figure 2.** Ball and stick drawing of  $((bz)CuCl_3)_2Zr(1)$  viewed down the **a** direction.

The benzene molecules are bound to the copper sites by an  $\eta^2$ -mode of coordination. Lying across the mirror plane, the benzene ligands are coordinated symmetrically to the copper atoms, with Cu–C distances of 2.306(7) Å and 2.200(6) Å for Cu(1) and Cu(2), respectively. The distance to the midpoint of the C–C bond (X) is Cu(1)–X(1) = 2.205 Å and Cu(2)–X(2) = 2.087 Å. In addition to the notable variation in bond distances to the respective benzene ligands, a distinct coordination geometry is also observed at Cu(1) and Cu(2) as seen in Figure 3. The benzene coordinated to Cu(1) forms a tetrahedron (based on the midpoint of the coordinated C–C bond) with the angles Cl(2)–Cu(1)–X(1) = 112.3° and Cl(1)–Cu(1)–X(1) = 114.3° and is oriented such that the ring lies over one of the three Cu–Cl bonds. By contrast, the coordination at Cu(2) is distorted toward a trigonal prismatic or nearly trigonal planar geometry with Cl(3)–Cu(2)–X(2) = 90.6° and Cl(4)–Cu(2)–X(2) = 129.5°. Here, the benzene is coordinated such that the ring lies over two of the three Cu–Cl bonds. The coordination to copper has apparently disrupted the aromaticity of both benzene ligands, although the errors in the C–C bond distances are too great to draw definitive conclusions. There is a qualitative difference

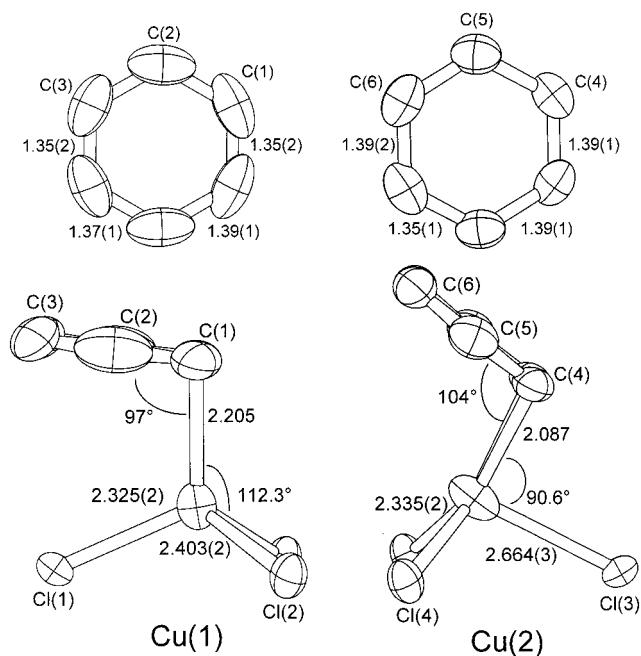


**Figure 3.** ORTEP drawings of the two distorted copper phosphonate-like building blocks in  $((bz)CuCl_3)_2Zr(1)$ .

in the C–C bond lengths of the benzene ligands coordinated to each copper (see Table 2 and Figure 3), which were consistently observed in the structural solution of the single-crystal X-ray diffraction data for two different crystals. The C(1)–C(1') bond, 1.35(2) Å, bound to Cu(1) is significantly shorter than the corresponding C(4)–C(4') bond, 1.39(1) Å, which is bound to Cu(2).

The zirconium octahedra are relatively idealized with six approximately equal Zr–Cl distances, avg Zr–Cl = 2.47 Å (Table 2). However, the significant differences between Cu(1) and Cu(2) are also seen in the dramatic variation in the copper–chloride bond distances (Figure 3). A 0.07 Å bond elongation of the two Cu(1)–Cl(2) bonds (2.403(2) Å), with respect to the Cu(1)–Cl(1) bond length of 2.325(2) Å, is observed at the Cu(1). (An average Cu<sup>I</sup>–Cl single bond distance is ca. 2.3 Å based on the sum of their crystal radii.)<sup>21</sup> By contrast, the Cu(2)–Cl(3) bond (2.664(3) Å) is elongated by 0.3 Å with respect to the two Cu(2)–Cl(4) bonds at 2.335(2) Å, where the elongated distance forms an axial-type coordination above a trigonal ligand plane.

(21) Shannon, R. D. *Acta Crystallogr.* **1976**, A32, 751.

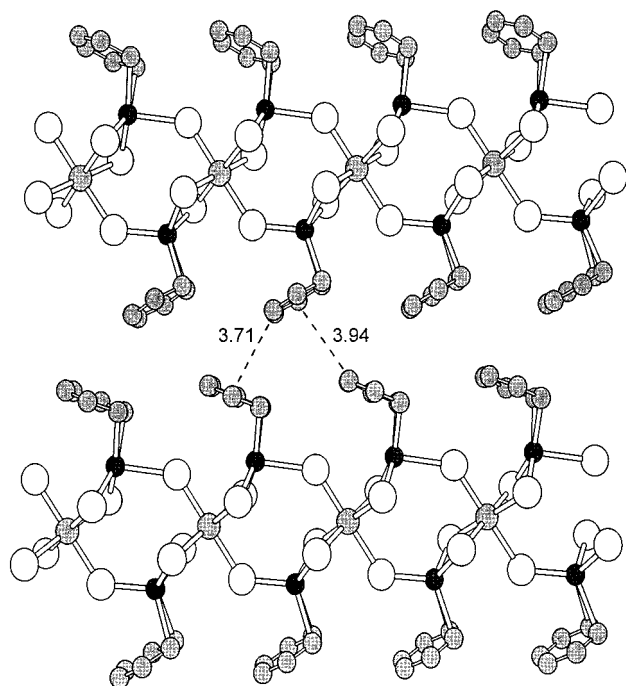


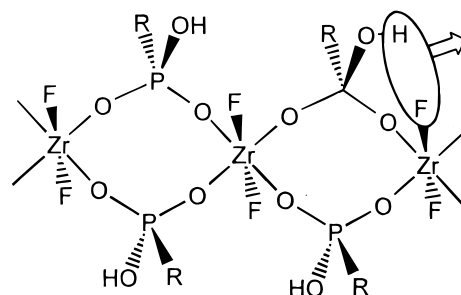
**Figure 4.** Ball and stick drawing of the chains in  $((bz)CuCl_3)_2Zr(1)$  stacked along the  $c$  direction to indicate the edge-to-face  $\pi$ -interactions between chains. Chlorides are the unshaded, larger balls. Zirconium atoms are the larger, gray balls, while carbon atoms are the smaller gray balls. Copper atoms are the darkest spheres shown.

The primary interchain interactions are observed by the stacking of the chains along  $c$  as shown in Figure 4. The edge of the benzene coordinated to Cu(1) is directed toward the face of the benzene ligand bound to Cu(2), and vice versa, such that short interchain contacts are observed, similar to that observed in the crystal structure of benzene itself.<sup>22,23</sup> The shortest interchain contacts are between the face of the benzene attached to Cu(2) and the edge of the benzene bound to Cu(1). (The face center to midpoint of C(3)–C(3') is ca. 3.71 Å.) The corresponding distance between the center of the face of the benzene attached to Cu(1) to the midpoint of the C(6)–C(6') bond is ca. 3.94 Å. Interestingly, there are no short contacts between the protons on the benzene ligands and the chloride ligands of neighboring chains. The shortest H...Cl distances are the intrachain contacts H(4)–Cl(3) = 2.92(2) Å, H(1)–Cl(2) = 3.14(2) Å and H(1)–Cl(1) = 3.35(2) Å. The shortest interchain H...Cl contacts are H(6)–Cl(4) = 3.001(2) Å and H(3)–Cl(2) = 3.03(1) Å, which only provide a weak link between chains along  $b$ .

## Discussion

**Synthesis.** Compound **1** is readily synthesized in high yield from the solvothermal reaction of  $Cu_2ZrCl_6$  in benzene. It is also possible to synthesize **1** directly from CuCl and  $ZrCl_4$  in superheated benzene. However, reactions starting with the binary halides normally result in a product with unreacted CuCl. Cuprous chloride is a very persistent species in both solvothermal and melt reactions, often requiring reactions to be heated to near its melting point to ensure complete reaction. Once the ternary  $Cu_2ZrCl_6$  is formed from the melt of the two binary

## Scheme 1



components, it is very amenable to further reaction in superheated benzene.

**A Metal Phosphonate Analog.** In a recent paper, we described the analogy between  $[CuCl_4]^{3-}$  and the thiophosphate  $[PS_4]^{3-}$ , where we demonstrated the structural relationship between  $[(ZrCl_2)CuCl_4]^{2-}$  and  $[MPS_4]^-$  ( $M = Ni,^{25} Pd^{26}$ ). On the basis of this same halide for chalcogenide charge matching scheme,  $[(bz)CuCl_3]^{2-}$  can be viewed as isoelectronic and isostructural to the phosphonate tetrahedral building blocks,  $[RPO_3]^{2-}$  ( $R = \text{alkyl or aryl}$ ). A search of the Cambridge Structural Database<sup>27</sup> finds no 1-D phosphonate for which **1** is a direct analogue. However, a close structural match is found for the 1-D phosphonate  $((RPO_3H)_2ZrF_2)^-$  ( $R = CH_2NH(CH_2CO_2)_2$ ) which was reported by Clearfield and co-workers and is shown in Scheme 1.<sup>28</sup> A figurative loss of HF would allow for the condensation to an edge-bridge phosphonate, which would then be a direct structural analogue to **1**. The absence of a direct phosphonate analogue to **1** is again understood because of the difference between the metal–oxygen and metal–chloride bond lengths.<sup>3</sup> The shorter M–O bond distance normally precludes the edge-shared type connectivity for octahedral and tetrahedral building blocks in the absence of metal–metal bonding. Though uncommon, edge-bridged connectivity between octahedral divalent metals and a phosphonate is observed for the 1-D chain structure of  $M^{II}(HO_3P(C_6H_5)) \cdot H_2O$  (where  $M = Ca, Mg, Mn,^{29} Zn^{30}$ ).

**Understanding the Structural Distortion of the Copper Tetrahedra.** Bonding interactions to copper(I) are known to be quite complex and varied.<sup>31</sup> The occupied  $3d^{10}$ -orbitals are of sufficient size and energy that  $\pi$ -back-bonding can be observed.<sup>4</sup> The empty  $4s$  and  $4p$  orbitals are rather low in energy, which allows copper(I) to act as an acceptor,<sup>32</sup> as well as facilitating distortions due to a second-order Jahn–Teller mixing into the occupied  $d$  levels.<sup>33</sup> The  $\eta^2$ -arene can also function as both a Lewis base or a Lewis acid, making use of its  $\pi$  and  $\pi^*$  orbitals, respectively.<sup>34</sup> Given the bonding interactions observed in the crystal structure of **1** with longer Cu(1)–C(1) and shorter

(22) Cox, E. G.; Cruickshank, W. J.; Smith, J. A. *Proc. R. Soc. London, Ser. A* **1958**, *247*, 1.  
 (23) Bacon, G. E.; Curry, N. A.; Wilson, S. A. *Proc. R. Soc. London, Ser. A* **1964**, *279*, 98.

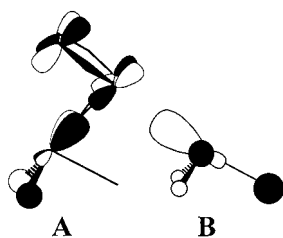
(24) Dattelbaum, A. M.; Martin, J. D. *Inorg. Chem.* **1999**, *38*, 2369.  
 (25) Chondoudis, K.; Kanatzidis, G.; Sayettat, J.; Jobic, S.; Brec, R. *Inorg. Chem.* **1997**, *36*, 5859.  
 (26) Elder, S. H.; Van der Lee, A.; Brec, R.; Canadell, E. *J. Solid State Chem.* **1995**, *116*, 107.  
 (27) 3D Search and REsearch Using the Cambridge Structural Database. Allen, F. H.; Kennard, O. *Chem. Design Automation News* **1993**, *8*, 1, 31.  
 (28) Zhang, L.; Poojary, D. M.; Clearfield, A. *Inorg. Chem.* **1998**, *37*, 249.  
 (29) Cao, G.; Lee, H.; Lynch, V. M.; Mallouk, T. E. *Inorg. Chem.* **1988**, *27*, 2781.  
 (30) Martin, K. J.; Squattrito, P. J.; Clearfield, A. *Inorg. Chim. Acta* **1989**, *155*, 7.  
 (31) Subramanian, L.; Hoffmann, R. *Inorg. Chem.* **1992**, *31*, 1021.  
 (32) Didziulis, S. V.; Cohen, S. L.; Butcher, K. D.; Solomon, E. I. *Inorg. Chem.* **1988**, *27*, 2238.  
 (33) Burdett, J. K.; Eisenstein, O. *Inorg. Chem.* **1992**, *31*, 1758.  
 (34) Harman, W. D. *Chem. Rev.* **1997**, *97*, 1953.

**Table 3.** Overlap Populations Calculated from Idealized  $(\text{bz})\text{CuCl}_3^{2-}$  Fragments

	Cu(1)		Cu(2)	
Cl(1)	0.3766	Cl(3)	0.334	
Cl(2)	0.3529 $\times$ 2	Cl(4)	0.3522 $\times$ 2	
C(1)–C(1')	1.0420	C(4)–C(4')	1.0356	
C(1)–C(2)	1.0659	C(4)–C(5)	1.0598	
C(2)–C(3)	1.0902	C(5)–C(6)	1.0915	
C(3)–C(3')	1.0702	C(6)–C(6')	1.0683	
total charge on Cu	11.0677		11.0317	

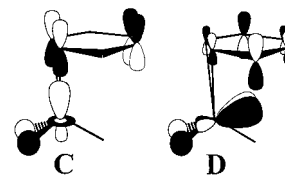
C(1)–C(1') bonds as compared to the shorter Cu(2)–C(4) and longer C(4)–C(4') bonds, one might suspect that each copper site exhibits a different bonding limit (ligand-to-metal or metal-to-ligand charge transfer). These bonding limits are readily articulated by a consideration of the frontier orbitals of the respective fragments.

The bonding distortions around Cu(2) are most pronounced and similar to those frequently observed for olefins coordinated to copper halides.<sup>35,36</sup> A second-order mixing of the higher-lying empty 4s and 4p orbitals into the occupied 3d orbitals on Cu drives a rehybridization that maximizes the possibility for  $\pi$ -back-bonding into the unsaturated ligand. Overlap for  $\pi$ -back-bonding is not well supported by a  $d^{10}$ -configuration in a tetrahedral geometry. However, distortion to the nearly trigonal-planar geometry observed around Cu(2) provides excellent overlap between the new  $\pi$ -type orbital on copper and a  $\pi^*$ -orbital of benzene shown in **A**. The formation of strong back-bonding into a  $\pi^*$ -orbital accounts both for the shortened Cu(2)–C(4) distance as well as for the lengthened C(4)–C(4') distance. The rehybridization on going to the near trigonal-planar geometry also serves to mix significant antibonding character into the Cu(2)–Cl(3) bond as seen in the decreased overlap population listed in Table 3. The empty 4s and 4p molecular orbitals on copper have significant Cu–Cl  $\sigma^*$  character, which when mixed into the former “ $t_2$ ”-type d-orbital of copper yields the molecular orbital **B**. Here, the second-order mixing has maximized antibonding to Cl(3), but is effectively nonbonding with respect to Cl(4). Hence, the rehybridization to maximize  $\pi$ -back-bonding to benzene comes at the expense of only one elongated copper-chloride bond.



A clearly different bonding motif is observed for Cu(1), which exhibits a more nearly ideal tetrahedral geometry and longer copper to benzene bonds. The larger thermal ellipsoids observed for this benzene ligand, though increasing the errors for the C–C distances, are also consistent with the weaker binding of this ligand. The C(1)–C(1') bond of the benzene ligand lies directly across one vertex of a tetrahedron with the plane of the ring essentially parallel to the three chloride ligands that make up its base. To a first approximation, the bonding of benzene to Cu(1) can be viewed as a result of the mixing of an empty  $sp$ -hybrid on copper with an occupied  $\pi$ -orbital of benzene and

the filled  $dz^2$  orbital on copper of the same symmetry (shown in **C**). The electron density transferred out of this  $\pi$ -bond is not sufficient to cause a significant lengthening of the C(1)–C(1') bond. But this analysis alone does not provide explanation for the elongation of two of the three Cu–Cl bonds by nearly 0.1 Å or the dearomatization of the coordinated benzene. To understand this distortion, we first note that unlike the distortion observed around Cu(2), this type of distortion does not have precedence in copper chloride olefin complexes. Unlike a simple olefin, benzene has several occupied  $\pi$ -type orbitals that may become involved in interacting with the metal center. While the primary  $\sigma$ -interaction with Cu(1) is formed with one  $\pi$ -orbital (shown in **C**), another of benzene's  $\pi$ -type orbitals is oriented so as to provide reasonable  $\pi$ -type overlap with one of the “ $t_2$ ”-type orbitals of the copper fragment shown in **D**. This metal-based orbital is  $\sigma$ -antibonding with respect to the two Cu(1)–Cl(2) bonds. Thus, this filled-filled interaction is stabilized by mixing with the empty Cu 4p-orbital. The strong Cu–Cl antibonding character of the Cu 4p orbital that is mixed into this occupied molecular orbital results in the elongation of two of the three Cu–Cl bonds (also seen in the overlap population listed in Table 3). This interaction also results in the decrease in the bonding angle of the plane of the benzene ring to the copper from 104° at Cu(2) to 97° at Cu(1), which appears to indicate a move toward a slightly greater hapticity ( $\eta^2 \rightarrow \eta^4$ ). Such a distortion cannot be observed for olefin complexes since olefins do not possess multiple occupied  $\pi$ -type orbitals. Furthermore, removing electron density from this “ $e_g$ ”-type  $\pi$  orbital of benzene (shown in **D**) is consistent with the observed dearomatization with longer adjacent C(1)–C(2) = 1.39(1) Å and C(2)–C(3) = 1.37(1) Å bonds and shorter C(1)–C(1') = 1.35(2) Å and C(3)–C(3') = 1.35(2) Å bonds.



The distinct coordination environments of the two copper sites in **1** reaffirm the precedent that the coordination sphere of copper(I) is quite flexible. The two bonding motifs seem clearly to be a result of ligand-to-metal charge transfer (for Cu(1)) and metal-to-ligand charge transfer (for Cu(2)). But why should these two distinct chemistries be present in this one structure? Looking beyond the bonding within the isolated chains, strong interchain interactions in the form of edge-to-face  $\pi$ -stacking of the benzene rings are apparent (Figure 4) that provide a significant influence in directing the charge transfer between metal and ligands. The partial negative charge on the face of an aromatic ring is frequently associated with the partial positive charge on the edge of a neighboring ring giving rise to substantial crystal packing forces. As noted above, and in Figure 4, the closest contact between the edge of the benzene ligand bound to Cu(1) and the center of the face of the benzene ligand bound to Cu(2) is 3.71 Å, which is slightly shorter than the distance of 3.75 Å found in the crystal structure of benzene itself. This interaction is favored by the respective charge transfer to and from the copper centers.<sup>22,23</sup> The ligand-to-metal charge transfer at Cu(1) depletes the electron density in the ring making a slightly more positively charged edge. By contrast, the metal-to-ligand charge transfer at Cu(2) increases the electron density, and thus the negative charge on the face of this ring.

(35) Hakansson, M.; Jagner, S.; Walter, D. *Organometallics* **1991**, *10*, 1317.

(36) Hakansson, M.; Jagner, S.; Clot, E.; Eisenstein, O. *Inorg. Chem.* **1992**, *31*, 5389.

## Conclusions

In summary, benzene is demonstrated to be a useful solvent for the solvothermal synthesis of metal-halide materials, such as  $((\text{bz})\text{CuCl}_3)_2\text{Zr}$  (**1**). The benzene coordinates to copper (I) forming the tetrahedral building block  $[(\text{bz})\text{CuCl}_3]^{2-}$ , which is recognized as an isostructural and isoelectronic metal-halide analogue of the metal-phosphonate unit  $[\text{RPO}_3]^{2-}$ . The chains formed in the crystal structure of **1** are oriented so as to exhibit edge-to-face  $\pi$ -stacking of the benzene rings, which promotes ligand-to-metal and metal-to-ligand charge transfer at Cu(1) and Cu(2), respectively. The ability for such interchain forces to direct the charge transfer between copper and the arene ligands bound to it imply that copper(I) can reasonably serve as an “electron buffer.” The dearomatization on coordination via metal-to-ligand charge transfer may make the aromatic ligand susceptible to electrophilic attack similar to that described for the  $\eta^2$ -arene complexes of osmium and ruthenium.<sup>34</sup> By contrast, the ligand-to-metal charge transfer should make the ligand

subject to nucleophilic attack as observed for the  $\eta^6$ -arene complexes of earlier transition metals.<sup>37</sup>

**Acknowledgment.** We would like to thank Ann E. Bunner for the contributions she made on this project as part of a summer high school research program and Dr. Paul Boyle for collecting the crystallographic data. This work was supported by the National Science Foundation CAREER award (DMR-9501370) and instrumentation grant (CHE-9509532). J.D.M. is a Cottrell Scholar of the Research Corp.

**Supporting Information Available:** An X-ray crystallographic file in CIF format for the structure determination of  $((\text{bz})\text{CuCl}_3)_2\text{Zr}$  (**1**). This material is available free of charge via the Internet at <http://pubs.acs.org>.

IC991064H

---

(37) Semmelhack, M. F. *Comprehensive Organic Synthesis*; Trost, B. M., Ed.; Pergamon Press: Oxford, 1990; Vol. 4, p 517.